

# Real-Time Monitoring Of Buried Oil Pipeline Right-Of-Way for Third-Party Incursion

Babatunde Olawale , Chris Chatwin, Rupert Young, Phil Birch

Department of Engineering and Design , University of Sussex, Brighton, United Kingdom

## Abstract

Many security systems employing different methods have been proposed to protect buried oil pipelines transporting petroleum products from the well-head via the refinery to: depots and other receiving stations. Currently there is a security gap in monitoring these buried pipelines in real time and in keeping them protected from third party interference. This paper addresses the problem of monitoring these systems by developing an automated image analysis system using an Unmanned Aerial Vehicle (UAV) equipped with sensors for monitoring buried pipeline-right-of-way (ROW). Video frame sequences captured by the UAV platform were ortho-rectified and mosaicked to form a seamless Digital Surface Model (DSM), which was then compared with an existing map for geo-referencing. This was achieved using the Direct Linear Transform (DLT) model and the Speed-up Robust Feature (SURF) algorithm. An OT-MACH correlation filter was applied to the geo-registered mosaicked video frames to detect third party interference with the ROW.

**Keywords:** *Correlation filters, Video mosaicking, Right-of-Way, Geo-reference, Pipeline, Unmanned aerial vehicle.*

## 1. Introduction

Many Unmanned Aerial Vehicle (UAV) technologies have been developed and used for military applications. These have led to useful applications in both the public and private sectors [1]. Among these sectors are aerial photography, agriculture, security, environmental, surveillance and monitoring [2]. Interference with pipeline Right-of-Way (ROW) is, typically caused by a third party using digging or drilling machines on the ROW, which can cause mechanical damage to the pipe or lead to problems ranging from pipe failure to explosion or environmental pollution. Since most of the reported damage to the pipeline ROWs are caused by third-party infringements [2, 3], the ability to detect third-party encroachment along the pipeline ROW will be a great benefit for pipeline monitoring and surveillance.

Many approaches have been used for monitoring and reporting third-party contact or activities along the pipelines; among these are the use of wired and wireless fiber-optic sensors buried alongside the pipe, satellite technology, manned aircraft, as well as foot and car patrols. All these methods have one limitation or another and, hence the need for alternative methods for monitoring the ROW.

This paper discusses how to automatically track pipeline right-of-ways, the detection of human tampering and/or theft and any type of third-party intervention.

Pipeline monitoring and threat detection are based on images taken from an autonomous UAV. The aim is to develop an automated image analysis system with the use of light UAVs for monitoring pipeline ROWs. This system should be able to identify potential hazards and vandals along the pipeline ROW automatically and send alerts to the pipeline response team in real-time. The major task to be solved is the detection of:

1. Human tampering and/or theft and any type of third-party intervention
2. Encroachment
3. Illegal refining

The technique used in this work is to lead the UAV to the pipeline ROW and arrange it to fly in a straight line along the ROW with the aid of a Global Positioning System (GPS). The UAV auto-pilot system is then programmed with four way-points to enable the UAV to keep tracking the pipeline ROW.

For the automatic analysis of this work, the Direct-Linear-Transform (DLT) model was used for ortho-rectification of individual video frames, and, the Speed-Up Robust Feature (SURF) algorithm was used for video frame mosaicking. The, Optimal Trade-off Maximum Average Correlation Height (OT-MACH) filter algorithm was used for object detection. The system is made up of the aerial platform and the ground station. The aerial platform consists of the UAV and sensors, which consist of a GPS, Inertial Navigation System (INS) and camera, all integrated into the UAV. The ground station consists of a portable PC computer and three servers, which comprise: an image processing application server, a threat database server and the base map server.

The UAV platform is responsible for data acquisition and the GPS and INS give the navigational position and attitude of the UAV, respectively. Data acquired are transmitted via a mobile communication data link to the ground station for processing.

At the ground station, the image processing application server, which contains the DLT model and the SURF

algorithm, are responsible for ortho-rectification of each video frame and ortho-frame mosaicking of all the frames, respectively. After the DLT algorithm has ortho-rectified each individual frame, the SURF algorithm aligns all the ortho-rectified video frames together to form a mosaic DSM covering the pipeline ROW. This module then hands over to the threat database server.

The threat database server module is responsible for detecting and identifying objects of interest on the pipeline ROW imagery that might represent a potential danger to the pipe. Here objects of interest are trained and stored in a database. Objects detected look for a candidate match in the database by the degree of matching with each object of interest in the database. A match indicates a threat and the image is then handed over to the base map server. This compares the DSM formed from the mosaic of video frames with an existing map in the base map database for geo-referencing and in order to determine the exact location of the threat found on the frame. If the object found could not find a match in the threat database then no other processing is required.

The base map server consists of an existing geo-referenced map of the pipeline ROW area. This base map must be updated once every three months in order to reduce mapping errors when comparing with the DSM formed from the mosaic

Once a threat is detected and its location known, an alert will be sent by the pipeline operator to the response team in real time.

The pipeline monitoring system used in this research is based on machine control vision. Machine vision was chosen because cameras are light and cheap. Also machine vision gives a tracking error which is directly related to the pipeline ROW, unlike GPS way-point control which gives tracking errors through a co-ordinate system fixed to the Earth[3]. The major contributions of this work are:

1. We were able to program the UAV auto-pilot system using four way points, which enable the UAV to fly along the required section of the pipeline ROW.
2. Our algorithms were tested with video collected on the UAV platform. They were able to perform video mosaicking on the ortho-images and detect objects of interest on the mosaicked video frames.
3. The detection algorithm was trained to detect object images by cropping and training the same object of interest under different illumination conditions.

## 2. Related Research

There are a number of technologies used for buried oil pipeline monitoring and threat detection. Most of these

technologies are based on using remote sensing to detect and report potential hazards [4]. These technologies depend on some types of communication networks which collect data and send alerts from inside and outside the buried pipe to the control station. Different types of network architecture have been used to provide effective communication in pipeline monitoring systems. These architectures, which are either wired or wireless networks or a combination of both networks, rely on factors such as power supplies and physical network security to be effective [5, 6, 7].

Fiber optic cables are used by wired networks for monitoring buried pipeline ROWs [8]. These cables are usually connected to sensor devices that measure the flow rate, the pressure and the temperature of the oil in the pipe [9,10]. The networks, which extend linearly along the pipeline, collect and send information from sensor nodes which spread over the pipeline to the control station [11, 12, 13, 14]. Wired network based monitoring systems are faced with the following types of problems:

1. If any wire in the network disconnects or is damaged, the whole pipeline monitoring system will be vulnerable to vandals.
2. The physical security of the system is not guaranteed when the pipeline extends over large areas.
3. Location and repairs of a faulty network can be very difficult since most of the pipelines are buried under-ground. Hence to maintain and repair a faulty network is a difficult task.
4. Repeated and irrelevant signals may be transmitted on the network causing delay for other relevant signals.

In order to overcome the short-comings of wired sensors [15, 16, 17] we have arrived at the idea of using wireless sensors to replace the wired sensors to monitor the buried pipeline system. In the wireless networks, the sensors which are distributed inside the buried pipe along the pipeline are divided into network segments. Unlike the wired sensors, if a sensor in a segment of the pipeline fails, due to damage to one of the sensors or any destructive action, the network is not affected because other sensors in the same segment or other segments will quickly detect the faulty sensor. The damaged sensor can then be physically replaced and new ones installed. The new sensor will automatically connect to the network segment without the need to program it into the sensor network. In the wireless sensor network, each sensor node acts as a communication relay node, such that each sensor node collects information from the nearest sensor node to it. The sensor node filters the sensed data and transfers it from one communication relay node to

another until it reaches a data dissemination node, which will then transfer it to the pipeline control station through another network. The problems with wireless sensors are:

1. If any node in the network develops a fault, the connectivity of the segment where the node belongs will be lost and the network is partitioned.
2. For pipelines that extend to large areas, a wide signal range will be needed for sensor nodes. This wireless range to stay connected will consume more energy from sensor batteries. This may lead to the requirement for frequent changes of sensor batteries.
3. Since most of the pipelines are buried under the ground, the task of maintaining the sensor network will be difficult.

Another technology used for oil pipeline monitoring and threat detection is satellite based technology. This technique utilizes pipeline and satellite data for surveying or providing surveillance of the pipeline. The satellite data is integrated with the pipeline data to produce a current pipeline map by using change detection analysis, i.e.; the current pipeline map is compared with a previous map to determine whether the route of the pipeline or the surrounding environment of the pipeline has changed. The satellite makes use of high resolution imagery as well as the pipeline data that includes location data, which is a series GPS coordinates [18, 19].

Satellite technology provides one of the most effective and efficient means for pipeline monitoring and threat detection. However, it is very expensive to build a satellite platform and sensor system, to launch it, to control it in its orbit and to recover data, as compared to operating a light aircraft with a good camera and scanner [20].

Also, for mapping to high accuracy over a relatively small area, data from sensors flown aboard an aircraft is much more useful than satellite data [18, 20]. Moreover, a satellite cannot take good quality images when the weather is cloudy. The fact that an unmanned aerial vehicle flies so much lower than satellites means that one can see more detail on the ground than can be obtained from commercial satellites.

The most widely used methods for pipeline monitoring include foot patrols along the pipeline ROW and aerial surveillance using helicopters. These patrols check for unauthorized intrusion into the pipeline ROW and leakages of the pipeline [19].

A disadvantage of this method arises from its cost and concern for the safety of the pilot flying at low altitude and during bad weather. The cost of foot patrols is high in terms of personnel and their time. The use of UAVs for

pipeline monitoring reduces operational costs, speeds up the process of monitoring and can be used in situations where manned inspection is not possible [20].

### 3. UAV System Overview

The UAV used in the experimental work reported in this paper is the Phantom 2 Quadcopter, which is a product of Djibouti Dow Jones (DJI) Industry Ltd, as shown in Fig.1. It is a lightweight, multi-functional integrated aircraft with a camera. Table 1, shows the main specification of the DJI Phantom 2 Quadcopter. The UAV consists of integrated GPS/INS for position, altitude control and auto-piloting which allows autonomous flight based on predefined way-points. The UAV supports up to 16 way-points in the flight plan



Fig. 1: DJI Phantom 2 Quadcopter Vision

The GPS/INS are integrated into the camera on board. This allows raw images captured to be linked to the exact location and time of acquisition of images. Since the Phantom 2 Vision has a camera integrated into the UAV, the tilt angle can be adjusted via the PC at the control station. The camera angle will move automatically to compensate the UAV's body tilting, giving more stable video footage. The Phantom 2 Vision gives real-time flight data and video feeds via Wi-Fi communication [21].

Table 1: DJI Phantom2 Vision specifications [21]

<i>AIRCRAFT</i>	<i>Battery</i>	<i>Flight Load Bearing</i>	<i>Hovering Accuracy(GPS Mode)</i>
	5200mAh Lipo	1160g	Vertical: 0.8; Horizontal:
	<i>Max Yaw Angular Velocity</i>	<i>Max Tilt Angle</i>	<i>Max Ascent/Descent</i>
	200 <sup>0</sup> /s	35 <sup>0</sup>	6m/s
	<i>Max Flying Speed</i>	<i>Diagonal Wheelbase</i>	<i>Tilting Range of Gimbal</i>
10m/s	350mm	0 <sup>0</sup> - 60 <sup>0</sup>	

The experiments were conducted on a pipeline right-of-way in Nigeria and a farm in the UK. Images of the right-of-way were captured from different elevations with the same configuration of the system. Tables 2 and 3 show the specification of the transmitter and camera employed.

Table 2: Transmitter specifications [21]

<b>TRANSMITTER</b>	<b>Operating Frequency</b>	<b>Communication Distance (open area)</b>
	5.8Hz15M	CE: 300m; FCC: 500m
	<b>Receiving Sensitivity</b>	<b>Transmitting Power</b>
	-93dBm	CE:25MW; FCC: 125mw
	<b>Working Current/Voltage</b>	<b>Battery</b>
	80mA/6V	4 AA Batteries

Table 3: Camera specifications [21]

<b>CAMERA</b>	<b>Resolution</b>	<b>FOV</b>	<b>Sensor Size</b>
	14Megapixels	140°/120°/90°	1/2.3
	<b>Functions</b>		
	<ul style="list-style-type: none"> <li>▪ Support of multi-capture, continuous capture and time capture.</li> <li>▪ Support of HD recording(1080p/10806</li> <li>▪ Support of both RAW and JPEG picture format</li> </ul>		

#### 4. General System Architecture and Workflow Chain

The system architecture and workflow chain is shown in Fig. 2. The system consists of an aerial platform and the ground station.

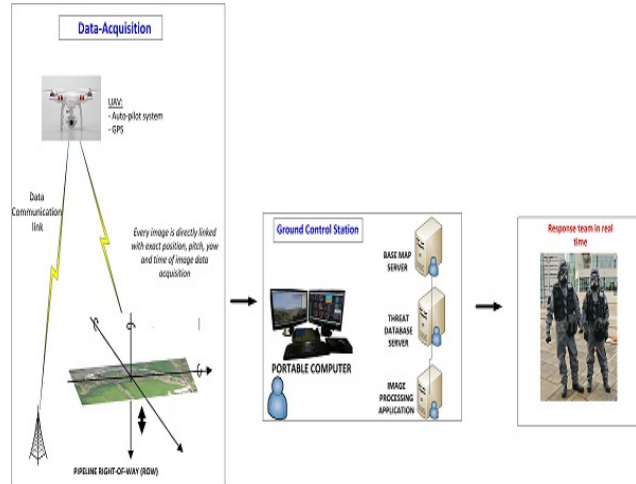


Fig 2 Architecture and workflow of the threat detection system

The aerial platform includes the UAV with a camera, the Global Positioning System and the Inertial Navigation System. The UAV which is equipped with an auto-pilot system, flies along the predefined pipeline ROW and acquires video imagery on the pipeline ROW. The video imagery is then transmitted to the portable PC at the ground station through a mobile communication data link in real time. In order to perform real-time image geo-referencing of the video stream acquired by the UAV platform, it is essential to generate a mosaic of images from the image sequence to allow for ortho-rectification. Due to the limited payload weight on the UAV platform we were forced to off-load this process to the ground station.

As mentioned in the introduction, the ground station consists of a PC with an image processing application server, threat database server and base map server.

The image processing application server receives the transmitted data from the UAV platform. Since the GPS and INS are integrated into the camera on board, the received video sequence frames are GPS/INS tagged (time and position tagged). The image application uses an algorithm to align GPS/INS tagged video frames from the video sequence together to form a single projective image view of the video scene. The final outcome of image alignment is a real-time geo-registered mosaic of images covering the pipeline ROW. The image processing application server then hands over to the threat database server.

The threat database server is responsible for detecting any objects of interest on the mosaic image, which may act as threats to the pipeline ROW. After objects are detected in the mosaic imagery, the image is handed over to the base map server for geo-referencing. The workflow is shown in Fig. 3.

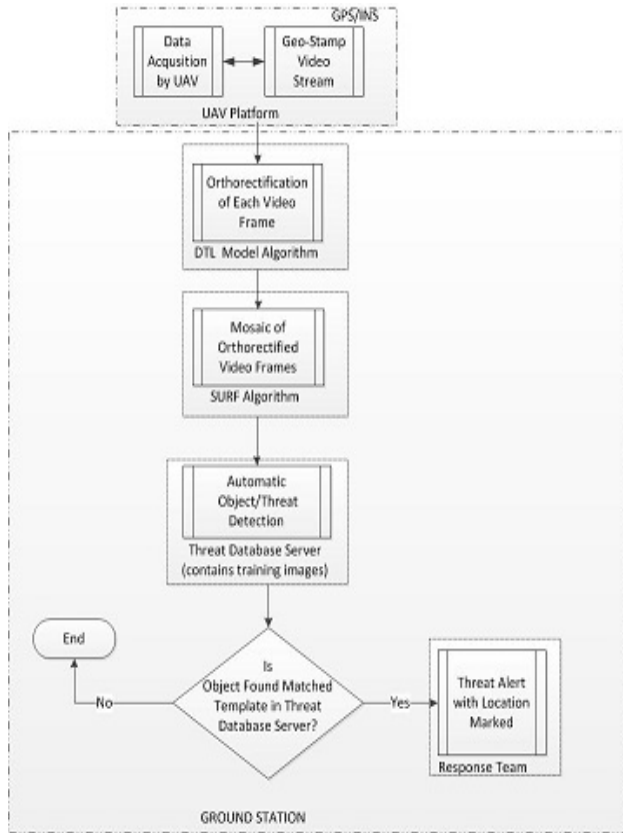


Fig. 3 Flow Chart of the threat detection system

## 5. Ortho-rectification and Geo-referencing

Ortho-rectification and geo-referencing are essential to pin point the exact location of targets in video image sequences acquired at the UAV platform. This can only be achieved by comparing such video imagery with an existing digital map. However, it is only when the image is ortho-rectified with the same coordinate system as an existing map that such a comparison is possible. The video image sequences from the UAV platform must be geo-registered, that is, each video frame must carry the necessary camera information in order to ortho-rectify the video frames. Then, many ortho-images(i.e. video frames) can be mosaicked together to form a seamless image map covering the pipeline ROW. This can then be used for comparison with an existing map for geo-referencing. In order to perform ortho-rectification on a video frame, the UAV video camera information, such as the intrinsic and the extrinsic parameters, must be known. The camera intrinsic parameters, which include; focal length;, principal point coordinates; and lens distortion calibration, can easily be determined during camera calibration before the flight. The major task is to get the extrinsic

parameters in real time, which requires knowing the position and attitude of the camera at the time image sequences are captured. The procedure for finding extrinsic parameters, called geo-referencing in this paper, tries to find the geometric relationship between video frames and the absolute ground coordinate system. The basic steps for video imagery geo-referencing are described in the following sub-sections:

### 5.1 Video Camera Calibration

The first step in geo-referencing is the calibration of the video camera(i.e. finding the intrinsic and extrinsic parameters of the camera), which allows for ortho-rectification of the individual video frames. For the calibration of the video camera, we used a mathematical model called the Direct Linear Transform(DLT), which was originally presented in [22]. This model is based on the principle of co-linearity(i.e. all points must be on a straight line), and it requires foreknowledge of the object space and image coordinates of a set of Ground Control Points(GCP). The DLT model can be expressed by:

$$x_1 - \Delta x = \frac{L_1 X + L_2 Y + L_3 Z + L_4}{L_9 X + L_{10} Y + L_{11} Z + 1} \quad (1a)$$

$$y - \Delta y = \frac{L_5 X + L_6 Y + L_7 Z + L_8}{L_9 X + L_{10} Y + L_{11} Z + 1} \quad (1b)$$

where coefficients  $L_1$  to  $L_{11}$  are the DLT parameters that reflect the co-linearity relationship between the 3D world object coordinates and the image plane( $x_1, y_1$ ),  $\Delta x$  and  $\Delta y$  are the optical errors and can be expressed as:

$$\Delta x = \varepsilon(L_{12}r^2 + L_{13}r^4 + L_{14}r^6) + L_{15}(r^2 + 2\varepsilon^2) + L_{16}\varepsilon\eta \quad (2a)$$

$$\Delta y = \eta(L_{12}r^2 + L_{13}r^4 + L_{14}r^6) + L_{15}\eta\varepsilon + L_{12}(r^2 + 2\eta^2) \quad (2b)$$

where,  $[\varepsilon, \eta] = [x - x_0, y - y_0]$  and  $r^2 = \varepsilon^2 + \eta^2$

In (2),  $L_{12} - L_{14}$  represent optical distortion while  $L_{15} - L_{16}$  represent de-centred distortion [22], as summarised in Table 4.

Table 4: Direct Linear Transform Parameters

Parameters	Remarks
$L_1 - L_{11}$	Standard DLT parameters
$L_{12} - L_{14}$	Optical distortion terms for 3 <sup>rd</sup> , 5 <sup>th</sup> , and 9 <sup>th</sup> order
$L_{15}$ and $L_{16}$	De-centred distortion term

With the use of iterative computation and the least square method, the 11 parameters can be determined. Then the intrinsic orientation and extrinsic orientation parameters can be calculated from the 11 determined parameters. In this way, the DLT model was used to determine the values of other vectors like the bore-sight matrix and the offset between the antenna and camera, etc. Detailed explanation of camera calibration is provided in [23].

### 5.2 Ortho-rectification of Video Frames

Each video frame can be ortho-rectified, after the orientation parameters of the individual video frame have been determined by the DLT model. Fig.4, shows the geometric relationship between the navigation sensors (i.e. GPS and INS), the video camera and the 3D world coordinates. The mathematical model for ortho-rectification of an individual video frame is given by [23]:

$$q_G^F = q_{GPS}^F(t) + Q_{INS}^F(t)[s_F * Q_C^{INS}(q_g^C(t) + q_{GPS}^C)] \tag{3}$$

where,  $q_G^F$  is a vector ground point G in the mapping frame,  $q_{GPS}^F(t)$  is a vector representing the GPS antenna phase centre in the mapping frame, (which is determined by the GPS at the UAV platform at a definite point in time(t)),  $Q_{INS}^F(t)$  is a rotational matrix from the INS body frame to the mapping frame and consists of three attitude rotation angles(i.e. roll, pitch and yaw),  $s_F$  represents the scale factor between the video frame and the mapping frame,  $Q_C^{INS}$  is called the bore-sight matrix, and represents the orientation offset between the camera frame and the INS body frame,  $q_g^C(t)$  is a vector in the image frame for point g, which is synchronised with the GPS periodic time t and  $q_{GPS}^C$  is the vector offset between the geometric centre of the GPS antenna and the camera lens centre.

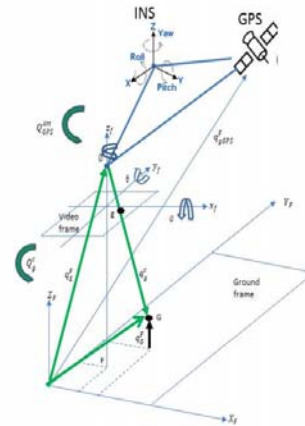


Fig. 4 Geometric Relationship between INS, GPS, video frame and the 3D world coordinates(modified from Guoqing [23] )

The next step after ortho-rectification of each video frame, is the mosaicking of all the ortho-images together to form a seamless map covering the entire pipeline ROW.

## 6. Real-time Video Mosaicking

In this research work, we used feature based video mosaicking techniques to mosaic all the ortho-rectified video frames formed in the previous section together. As described in the previous section, this operation was outsourced to the ground station in the image processing application server because of its high computational requirements. We chose the feature based video mosaicking approach because it has clearly defined advantages based on good performance gains with respect to camera movement, better inter-frame overlapping and easy identification of breaks in the continuity of video frame sequences [24]. Also, from empirical results, a feature based approach appears to perform well in re-registration after a break in continuity of the incoming video sequence [24].

### 6.1 Speed-Up Robust Feature(SURF)

For video mosaicking, SURF operates by identifying distinct feature points within individual video frames. These feature points are then used to extract a set of matches between successive frames. Next, the RANSAC based method is used to remove statistical outliers and to constantly check for the consistency of the detected set of

matches. Afterwards, bundle adjustment is used to estimate the image alignment. A 3D visualization [25] was used to produce a mosaic of images from the captured video frame sequences and their estimated alignment.

## 6.2 Feature Point Detection

Feature points are selected at distinctive locations on the captured video frames, such as corners, blobs and T-junctions. The SURF feature point detector is invariant to scaling, rotation and partially sensitive to change in illumination. Much research has been done on feature detection and description, a detailed comparison and analysis being presented, for example, in [25].

## 6.3 Feature Matching and RANSAC model

Within the task of video mosaicking, successive video frame sequences are made to overlap and aligned to form a mosaic image of the video scene. The SURF algorithm was used to perform the video mosaicking. The algorithm first identifies the corners in the first and second frame using the first frame as the reference frame. It then, calculates the affine transformation matrix that best describes the transformation between corner positions in these frames [26]. Finally, the algorithm matches the second frame onto the first frame. This process is repeated until all the video frames are aligned together. Two frames are matched (i.e. their feature vectors are matched) if the Euclidean distance between them is less than the threshold set by the match threshold parameter. The feature vector  $x$  from the first frame is considered a match to the feature vector  $y$  from the second frame if their Euclidean distance  $ED$  satisfies the following relationship:

$$\frac{ED}{ED_{all}} < \text{thres} \quad (4)$$

where  $ED_{all}$  is the minimum difference over all possible differences between feature vector  $x$  and every feature vector, which excludes feature vector  $y$ . The threshold,  $\text{thres} = 0.34$ , was chosen, with other lower and higher values giving false matches. A RANSAC model of a 3x3 projective transform matrix was chosen to identify and pass only the statistical inliers in the final stage, which is frame alignment using the bundle adjustment. More details on video mosaicking using SURF can be found in [25, 26].

## 7. Object Detection

We used a composite correlation filter algorithm in this experiment for object detection because of its ability to handle general types of distortion. Also, since it is a Correlation Pattern Recognition (CPR) filter, it has the robust property of evaluating the whole input signal at once, unlike the feature-based techniques, which minutely extract information from piecewise examination of the signal and compare the relationships between the features [25]. Matching the whole image against the template makes the CPR less sensitive to small mismatches [26]. Composite correlation filters are designed from many training images, which represent the different views of the objects to be detected [25, 26]. The filter can be trained to detect and recognise any object with any kind of distortion as long as the expected variations can be captured by the training images [27]. The major aim of all composite filters is to be able to recognise the object on which they were trained. To obtain a cross-correlation as a function of the relative shift between a query image and a set of training image templates, the query image is compared to the template. The whole operation is computed in the spatial frequency domain for computational efficiency by performing the complex multiply:

$$Y(a,b) = X(a,b) H^* (a,b) \quad (5)$$

where  $X(a,b)$  is the 2D-Discrete Fourier Transform (DFT) of the query image,  $H(a,b)$  is the spectrum of the reference template,  $*$  denotes the complex conjugate of the filter spectrum and  $Y(a,b)$  is the DFT of the correlation output  $y(m,n)$ . A Fast Fourier Transform (FFT) algorithm is used to implement the DFT efficiently. Whenever there is a match between the query image and the template image, the correlation filters are designed to give a sharp peak at the centre of the correlation output plane and no peak if there is no match between the query image and the template image, as illustrated in Fig. 4.

The composite correlation filter, used in this research, is the Optimal Trade-off Maximum Average Correlation Height (OT-MACH) filter. The first composite correlation filter developed, was the Projection Synthetic Discriminant Function filter (PSDF) [28]. However, PSDF filters suffer from not having any in-built robustness to noise and display large side lobes, making location of the correlation peak difficult. The Minimum Variance SDF (MVSDF) [28] was then developed to minimise the Output Noise Variance (ONV) in the

projection SDF. The MVSDF is able to improve correlation peak height variations but cannot

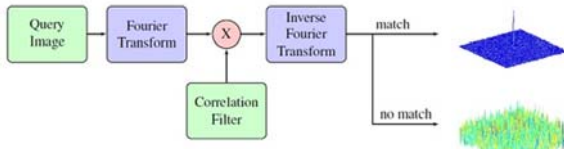


Fig. 4: Matching (correlating) a query image with the template (correlation filter)

suppress white noise. In order to solve the problem of white noise and high correlation peak side lobes generated by the earlier composite correlation filters, the Minimum Average Correlation Energy(MACE) [28] filter was developed. The MACE filter is able to suppress the side lobes and produce sharp correlation peaks but is still not as robust to noise as the MVSDF. The two filters the MVSDF and MACE, can be combined and used if there is only one training image. The MACE filter is used as the inverse filter, while the MVSDF filter is used as the matched filter since both attributes are needed to produce sharp peaks and at the same time suppress noise. It was discovered by the authors of [27, 28] that both attributes can be integrated into a single filter by providing an optimal trade-off between the MACE and the MVSDF. To illustrate the optimal trade-off between these filters, let us consider the design of a filter that uses two performance criteria, the ACE and ONV, in order to satisfy a set of linear constraints. ONV is minimized for every possible choice of ACE, since it is not possible to minimise both criteria. This is illustrated in the following Lagrangian function:

$$\phi(\rho) = ONV - \rho(ACE) - h^+ X\delta \quad (6)$$

where  $\rho$  is a single Lagrange multiplier that forces ACE to a fixed value,  $\delta$  is the vector of M Lagrange multipliers, which corresponds to the linear constraints on the correlation peaks in response to M training images. It can be seen that when ACE is fixed to any value, minimising  $\phi(\rho)$  will also minimize ONV.

If :

$$\rho = \frac{(\mu - 1)}{\mu} \in [0,1], \quad (7)$$

i.e. the Lagrangian function,

equation (6) becomes:

$$\phi(\mu) = \mu\phi(\rho) = \mu ONV + (1 - \mu)ACE - h^+ X_q \quad (8)$$

where  $q = \mu\delta$ . Hence, the weighted linear combination of ACE and ONV indicates the performance criterion to be minimised.

This approach can be applied to more than two performance criteria and to other unconstrained correlation filters like the MACH filter [27]. When the optimal trade-off performance criterion is applied to the MACH filter, it takes the form:

$$h = (\alpha ACE + \beta ASM + \gamma ONV)^{-1} m \quad (9)$$

where  $\alpha$ ,  $\beta$  and  $\gamma$  are the optimal trade-off parameters, which are associated with the performance criteria ACE, ASM and ONV, respectively. Each parameter is varied while all others are held constant until a satisfactory value is found. A detailed explanation of the OT-MACH filter is given in [26, 27, 28, 29].

## 8. Experimental Results

Fig. 6(a) is the raw video stream captured by the UAV on the pipeline ROW with the target object in view. Each video frame of the raw data is then ortho-rectified individually and, these ortho-images are then mosaicked together by the SURF algorithm. The result obtained is shown in Fig 6(b).

Fig.7 shows the trained images, which are images of interest. They are trained for different viewing angles from  $0^0$  to  $140^0$ . In Fig. 7(a) the training image in Fig 7(b) is a person.

The OT-MACH filter algorithm was applied to the mosaic of ortho-images formed in Fig. 6(b) and the result obtained, shown in Fig. 8(a), which shows that there is a correlation between one of the training images and the target image found on the pipeline ROW. The corresponding correlation response with a sharp peak is displayed in Fig. 8(b) indicating the presence of the object of interest. Fig. 8(c), shows an ortho-image containing an object of interest viewed at an angle of  $60^0$  by the UAV and Fig. 8(d) shows the result after the application of the detection (by the OT-MACH filter) algorithm while the sharp peak in Fig. 8(e) indicates that an object was detected by the filter.



(a)

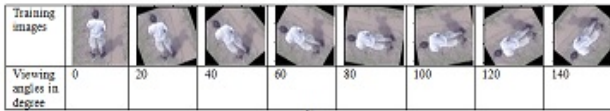


(b)

Fig. 6 Video Mosaicking by SURF algorithm (a) Video stream of target before mosaicking (b) mosaic of images formed from the video stream



(a)

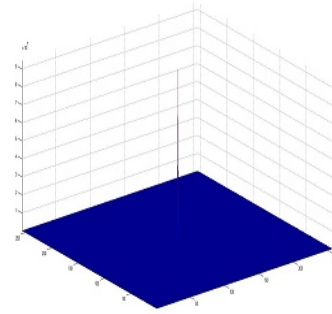


(b)

Fig. 7 (a) training images for a car (b) training images for a person



(a)



(b)

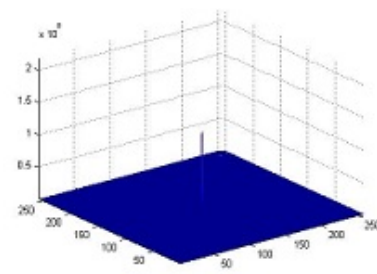
Fig. 8 Object Detection by OT-MACH filter algorithm (a) Object detected on mosaic image (b) Correlation response with a sharp peak meaning an object detected (c) Ortho-image from UAV (d) object detected from viewing angle of  $60^{\circ}$



(c)



(d)



(e)

## 9. Conclusions

The paper has proposed an automatic aerial monitoring system using a combination of the DLT model, SURF, and OT-MACH filter algorithms for video frame orthorectification, video frame mosaicking, and object detection, respectively. The performance has been evaluated experimentally and has shown promising results in terms of detection and positioning accuracy. The current implementation of the algorithms runs at 6.25 Hz on a standard desktop core i7 PC, indicating that this approach is suitable for real-time use on-board a small aerial platform/UAV.

## References

- [1] J. Allen, and B. Walsh, "Enhanced Oil Spill Surveillance, Detection and Monitoring through the Applied Technology of Unmanned Air Systems". In: *Proceedings of the 2008 international oil spill conference*.
- [2] M. Bertalmio, L. Uminita, G.S. Vese, and S.S. Osher, "Simultaneous Structure and Texture Image Inpainting", *IEEE Transactions On Image Processing*, vol. 12, No. 8, **2003**.
- [3] B. Colfman, M. McCord, and K. Redmill, "Surface Transportation Surveillance from Unmanned Aerial Vehicles" *Proc. Of the 83<sup>rd</sup> Annual Meeting of the Transportation Research Board*, **2004**.
- [4] P. Baronti, P. Pillai, V. Chook, S. Chessa, F. Gotta, and H. Fun, "Wireless sensor networks: a survey on the state of the art and the 802.15.4 and zigbee standards". *Communication Research Centre, UK*, May **2006**
- [5] A. Carrillo, E. Gonzalez, A. Rosas, and A. Marquez, "New distributed optical sensor for detection and localization of liquid leaks". *Pat I. Experimental Studies, Sensorss, Actuators*, A(99):229–235, **2002**.
- [6] C. Chong, and S.P. Kumar, "Sensor networks: Evolution, opportunities, and challenges". *Proceedings of the IEEE*, 91(8), August **2003**.
- [7] IEEE P802.15.4 / D18. Low rate wireless personal area networks. **2003**.
- [8] S. De, S.K. Das, H. Wu, and C. Qiao, "A resource efficient RTQoS routing protocol for mobile ad hoc networks". *Wireless Personal Multimedia Communications, 2002. The 5th International Symposium on*, 1:257–261, **2002**.
- [9] N. Mohamed, and I. Jawhar, "A Fault-Tolerant Wired/Wireless Sensor Network Architecture for Monitoring Pipeline Infrastructures". In *Proceedings of the Second International Conference on Sensor Technologies and Applications (SENSORCOMM 2008)*, Cap Esterel, France, 25–31 August **2008**; pp. 179-184.
- [10] Y. Tu, and H. Chen, "Design of oil pipeline leak detection and communication systems based on optical fiber technology", *Proc. SPIE* **1999**, 3737, 584-592.
- [11] W. Lin, "Novel distributed fiber optic leak detection system", *Opt. Eng.*, **43**:278–279, **2004**.
- [12] I. Jawhar, N. Mohamed, M. Mohamed, and M.A. Aziz, "Routing Protocol and Addressing Scheme for Oil, Gas, and Water Pipeline Monitoring Using Wireless Sensor Networks". In: *Proceedings of the Fifth IEEE/IFIP International Conference on Wireless and Optical Communications Networks(WOCN2008)*, Surabaya, East Java, Indonesia, 5–7 May **2008**.
- [13] H. van der Werff, M. van der Meijde, F. Jansma, F. van der Meer, G.J. Groothuis, "A spatial-spectral approach for visualization of vegetation stress resulting from pipeline leakage", *Sensors* **2008**, 8, 3733-3743
- [14] N. Mohamed, I. Jawhar, "A Fault-Tolerant Wired/Wireless Sensor Network Architecture for Monitoring Pipeline Infrastructures". In: *Proceedings of the Second International Conference on Sensor Technologies and Applications (SENSORCOMM 2008)*, Cap Esterel, France, 25–31 August **2008**; pp. 179-184
- [15] A. Carrillo, E. Gonzalez, A. Rosas, and A. Marquez, "New distributed optical sensor for detection and localization of liquid leaks: Part 1—Experimental studies". *Sens. Actuat. A* **2002**, 99, 229-235.
- [16] W. Lin, "Novel distributed fiber optic leak detection system". *J. Opt. Eng.* **2004**, **43**, 278-279.
- [17] I. Stoianov, L. Nachman, S. Madden, and T. Tokmouline, "PIPENET: A Wireless Sensor Network for Pipeline Monitoring". In *Proceedings of the 6th International Conference on Information Processing in Sensor Networks*, Cambridge, MA, USA, 25-27 April **2007**; pp. 264-273.
- [18] Y. Jin, and A. Eydgahi, "Monitoring of Distributed Pipeline Systems by Wireless Sensor Networks". In *Proceedings of the International Conference on Engineering and Technology*, Nashville, TN, USA, 17–19 November **2008**.
- [19] F. Murphy, D. Laffey, B. O'Flynn, J. Buckley, and J. Barton, "Development of a wireless sensor network for collaborative agents to treat scale formation in oil pipes". *LNCS* **2007**, 4373, 179-194.
- [20] Anon, "Functional Specification For a Satellite Surveillance System", Andrew Palmer and Associates Report NR01003, March **2001**.
- [21] <http://www.wiki.dji.com> (Accessed: 11 July **2013**).
- [22] Y.I. Abdel-Aziz, and H.M. Karara, "Direct linear transformation from comparator coordinates into object space coordinates in close-range photogrammetry," in *Proc. Symp. Close-Range Photogramm.*, 1971, pp. 1–18.
- [23] Z. Guoqing, "Near Real-Time Orthorectification and Mosaic of Small UAV Video Flow for Time-Critical Event Response" In proceeding on Geoscience and Remote Sensing, *IEEE*, 47(3), March **2009**
- [24] M. Brown, and B. Lowe, "Automatic Panoramic Image Stitching using Invariant Feature". *International Journal of Computer Vision*, 74(1):59{73, Aug. **2007**.
- [25] H. Bay, A. Ess, T. Tuytelaars, and L. Van Gool "Speeded-Up Robust Features (SURF)". *Computer Vision and Image Understanding*, 110(3):346 - 359, **2008**.

- [26] J. Juan, and O. Gwun, "A comparison of SIFT, PCA-SIFT and SURF". International Journal of Image Processing, 3(4):143-152, July/August 2009.
- [27] Ph. Refregier, "Optimal trade-off filters for noise robustness, sharpness of the correlation peak and Horner efficiency", Optics Letters, Vol. 16, No. 11, 829-831, 1991
- [28] B.V.K. Vijaya, A. Mahalanobis and R.D. Juday, "Correlation pattern recognition". Cambridge university press USA, 2005, pp196-243.
- [29] L.S. Jamal-Aldin, R.C.D. Young, and C.R. Chatwin, "Application of nonlinearity to wavelet-transformed images to improve correlation filter performance", Applied optics 36 (35), 9212-9224, 1997

**Babatunde Olawale** is a current doctoral post graduate student at the university of Sussex, United Kingdom. He had his first degree in (B.Tech) Computer Engineering in the year 2000. He has three different post graduate degrees in the following fields – Master in information Technology in the year 2005, Master in Computer Science in the year 2007 and Master in Security Systems and Technology in the year 2011. He is a lecturer at the Osun state polytechnic, Nigeria since 2001 to date. His research areas are : Computer vision, image processing, remote sensing and pattern recognition

**Professor C. R. Chatwin** holds the Chair of Engineering, University of Sussex, UK; where, *inter alia*, he is Research Director of the "iisp Research Centre." and the Laser and Photonics Systems Engineering Group. At Sussex has been a member of the University: Senate, Council and Court. He has published two research monographs: one on numerical methods, the other on hybrid optical/digital computing - and more than two hundred international papers. Professor Chatwin is on the editorial board of the International Journal "Lasers in Engineering". He is also a member of: the Institution of Electrical and Electronic Engineers; IEEE Computer Society; the British Computer Society; the Association of Industrial Laser Users, European Optical Society. He is a Chartered Engineer, Euro-Engineer, International Professional Engineer, Chartered Physicist, Chartered Scientist and a Fellow of: The Institution of Electrical Engineers, The Institution of Mechanical Engineers, The Institute of Physics and The Royal Society for Arts, Manufacture and Commerce

**Rupert Young** is a reader at the Department of Engineering and Design, University of Sussex United Kingdom. He graduated from Glasgow University where he gained his PhD in Coherent Optical Signal Processing. He is a member of the Society of Photo-optical and Instrumentation Engineers. He is also a member of Optical Society of America. His present research areas are Computer Vision & Image Processing -Pattern Recognition, Computer Vision and Image Processing - Security, Genetic Algorithms (CS), Holography Instrumentation, Medical Informatics, Photonics.

**Phil Birch** completed his PhD at the University of Durham in 1999 on Liquid Crystal Devices in Adaptive Optics. The systems built used various liquid crystal spatial light modulators (SLMs) to correct for phase aberrations introduced by atmospheric turbulence. This is important for astronomical imaging and free space optical communications. Phil has worked in industry developing rapid prototyping equipment and optical metrology systems. Since working at the University of Sussex he has been researching COMPUTER generated holograms (CGH), correlation pattern matching, and optical microscopy. He has also worked with industrial partners in image processing, object detection and tracking.